NanoImpact 10 (2018) 161–167

Contents lists available at ScienceDirect

NanoImpact

journal homepage: www.elsevier.com/locate/nanoimpact

Frontier article

Towards reproducible measurement of nanoparticle size using dynamic light scattering: Important controls and considerations

D. Langevin[a,*], E. Raspaud[a], S. Mariot[a], A. Knyazev[a,1], A. Stocco[a,2], A. Salonen[a], A. Luch[b], A. Haase[b], B. Trouiller[c], C. Relier[c], O. Lozano[d,3], S. Thomas[e], A. Salvati[e,f], K. Dawson[e]

[a] Laboratoire de Physique des Solides, CNRS, Univ. Paris Sud 11, Université Paris Saclay, 91405 Orsay, France
[b] German Federal Institute for Risk Assessment, Department of Chemical and Product Safety, 10589 Berlin, Germany
[c] Ineris, Parc Technologique Alata, BP2, 60550 Verneuil en Halatte, France
[d] Namur Nanosafety Centre (NNC), Namur Research Institute for Life Sciences (NARILIS), Research Centre for the Physics of Matter and Radiation (PMR), University of Namur, Namur, Belgium
[e] Centre for BioNano Interactions, University College Dublin, Belfield, Dublin 1, Ireland
[f] Groningen Research Institute of Pharmacy, University of Groningen, 9713AV Groningen, The Netherlands

ABSTRACT

The characterization of nanoparticles in dispersions, in particular measuring their size and size distribution, is a prerequisite before they can be used in toxicological testing. Such characterization requires reliable methods with good reproducibility. The aim of this study was to evaluate the reproducibility, and thus the potential of Dynamic Light Scattering (DLS) for nanoparticle size determination. DLS is easy to use and well established in most nanotoxicology laboratories. However, reproducibility and in particular variability between measurements done using different instrumental setups have not been addressed systematically before. Here we performed initial experiments with rather monodisperse dispersions of spherical particles in water. Significant discrepancies in the measured distributions were obtained with different DLS instruments, especially when fitting the data using mathematical inversion methods. Significant errors can be made due to different settings being used for fitting the data. These were even more prominent when working with dilute dispersions of very small particles. Our study has identified several important points to be taken into consideration in order to overcome possible issues in measurement and analysis of nanoparticles using DLS.

In practice, however, nanoparticles may have significant polydispersities and/or can be non-spherical. We extend the comparative work on spherical particles, to show how to characterize polydisperse and/or high aspect ratio particles using DLS instruments.

1. Introduction

The impact of nanoparticles on living systems is an important issue. The potential toxicity of nanoparticles was found to depend not only on their size and shape, but also on the particle material and coating, its porosity, crystallinity, heterogeneity, roughness and even strain of bonds between surface groups; other parameters such as dissolution rate and dispersion state were also found important (Nel et al., 2009; Zhang et al., 2012; Wang et al., 2013; Anguissola et al., 2014; Guarnieri et al., 2014; Sabella et al., 2014; De Matteis et al., 2015). In addition, transport over the course of in vitro exposure to cells plays an important role (DeLoid et al., 2017; Beltran-Huarac et al., 2018). The characterization of nanoparticles in dispersions, in particular measuring their size and size distribution, is a prerequisite before they can be used in toxicological testing, and in scientific studies of biological interactions. The size characterization is very basic for all such studies and therefore requires reliable methods with good reproducibility. A well-used method is dynamic light scattering (DLS), which principle is briefly recalled below.

Due to Brownian motion, a nanoparticle liquid dispersion is not fully homogeneous, some regions contain more particles than others at a given time. When exposed to an incident light beam, the particles scatter the light and, as a result of their motion, a spectral broadening due to the Doppler Effect occurs. The broadening is of order of D/λ^2,

* Corresponding author.
E-mail address: dominique.langevin@u-psud.fr (D. Langevin).
[1] present address: Global QC MI&S Shire, Route Pierre-à-Bot 111, 2000 Neuchâtel, Switzerland.
[2] present address: Laboratoire Charles Coulomb, CNRS, Université Montpellier, Montpellier, France.
[3] present address: Cátedra de Cardiología y Medicina Vascular, Escuela de Medicina y Ciencias de la Salud, Tecnologico de Monterrey, Monterrey, Mexico.

https://doi.org/10.1016/j.impact.2018.04.002
Received 7 February 2018; Received in revised form 5 April 2018; Accepted 5 April 2018
Available online 10 April 2018
2452-0748/

with D the particle diffusion coefficient and λ the wavelength of light (Kerker, 1969). For nanoparticles of 20 nm radius in water and a wavelength of 600 nm, this broadening is of the order of 1000 Hz, whereas the typical light frequency is 10^{14}–10^{15} Hz. In order to detect such a small broadening, monochromatic laser sources should be used. By measuring the broadening of laser spectral lines, or alternatively the time correlation function of the scattered intensity, the diffusion coefficient D can be determined. From D, the particle size can be obtained. This method is called Dynamic Light Scattering (DLS) (Berne and Pecora, 2000). DLS was developed in the 1960s and 70s, after lasers became available. Today, many different commercial setups exist and machines can be purchased from various vendors. Most popular are benchtop instruments, which often are able to determine not only the size of the particles, but also their zeta potential. Such instruments are nowadays extensively used in standard characterization laboratories as well as in many toxicological/ biological laboratories because they are simple to operate and not too expensive. However, if the measurements are automatized to a large extent, users need to be well aware of important controls and potential sources of errors in size determinations. Overall, when measuring spherical particles with well defined, monomodal size distributions, DLS can give reliable results provided the measurement and the data analysis are performed with care.

However, when measuring polydisperse particles and/or non-spherical particles, more sophisticated instruments are needed. In particular, as the intensity of the light scattered by particles increases as the sixth power of the diameter and the signal is dominated by the largest particles: this means that when the dispersions contain both large and small particles, the small ones can hardly be detected.

The present paper aims to carefully elucidate potential issues that if overlooked, lead to errors in measuring nanoparticle size with DLS. A particular focus was laid on data analysis using multiple algorithms that are currently available. To that end we tested only a limited number of rather ideal nanoparticles (i.e. spherical particles with monomodal size distribution). Also we would like to emphasize that our goal was not a systematic evaluation or comparison of different commercial instruments but rather we randomly selected a few examples representing the variety of currently used instruments. Thus, the aim of this study was to raise user awareness for different critical issues that can occur when using DLS and to provide a guidance in particular for those users that are less trained in nanoparticle characterization but have the possibility to use such instruments alongside with their toxicological studies. We show that there are several important points to take into account in order to obtain reliable results, such as for instance limiting the range of correlation times. We also propose solutions for robust nanoparticle characterization.

2. Principle of the method

We will briefly recall below the principle of DLS data analysis. Useful complementary information and practical details can be found for instance in (Russo, 2012). As explained in the introduction, the Brownian motion of particles produces fluctuations of the scattered light intensity. The DLS instruments measure in general the correlation function of the scattered intensity I: $g_2(\tau) \leq I(t)\ I(t+\tau) > / < I(t)^2 >$, where t is the time and τ is the lag time, which is adjustable.

In the ergodic limit (space and time averages identical), this correlation function is related to the correlation function for the scattered electric field E, $g_1(\tau) = < E(t)\ E(t+\tau) > / < E(t)^2 >$ through the Sigert relation: $g_2(\tau) = 1 + \beta g_1(\tau)^2$, where β is an instrumental parameter ($0 < \beta < 1$).

2.1. Monodisperse spherical particles

When the particles are spherical and monodisperse:

$$g_2(\tau) = 1 + \beta \exp(-\tau/\tau_D) \tag{1}$$

with

$$\tau_D = 1/(2Dq^2) \tag{2}$$

D being the diffusion coefficient and q the wave vector: $q = 4\pi n \sin(\theta/2)/\lambda$, with θ the scattering angle, n the solution refractive index and λ the wavelength of light. If the dispersions are dilute so that interactions between particles can be neglected, D is given by the Stokes-Einstein formula:

$$D_{st} = \frac{k_B T}{6\pi\eta R_h} \tag{3}$$

k_B being the Boltzmann constant, T the absolute temperature, η the viscosity of the liquid used to disperse the particles and R_h their hydrodynamic radius.

In some DLS instruments, a goniometer allows to systematically vary the scattering angle θ, hence the wave vector q. The validity of Eq. 2 can then be checked, proving that the particle motion is Brownian, and very precise values of the diffusion coefficient and particle size are obtained. In simpler instruments, the detector is fixed, usually in backscattering conditions ($\theta \sim 170°$). Therefore, the eventual influence of convection cannot be evaluated and the accuracy on the particle size is lower.

When the dispersions are not dilute, interactions between particles start playing a role and D differs from the Stokes expression: D is larger for repulsive particles and smaller for attractive ones. For dispersions containing only a few volume percent of particles:

$$D \sim D_{st}\ (1 + \alpha\, \phi) \tag{4}$$

ϕ is the particle volume fraction. In the special case of hard-sphere interactions $\alpha \sim 1.5$ (Russel, 1981). In general α is of order of unity, so little error is made calculating the particle radius with the Stokes formula provided the volume fraction is below or around 1%.

2.2. Polydisperse spherical particles

In practice, particles are never monodisperse, and the correlation function is a superposition of functions corresponding to the different particle sizes. When the polydispersity is not too high, the correlation function can be written as a *cumulant* expansion:

$$ln\left[g_2(\tau) - 1\right] \cong -\frac{\tau}{\tau_D} + \frac{\mu_2}{2}\left(\frac{\tau}{\tau_D}\right)^2 \tag{5}$$

where $\mu_2/2$ is the polydispersity index (PDI). For a Gaussian size distribution with a mean size $\overline{R}$:

$$f(R) = \frac{1}{\sigma\sqrt{2\pi}}\, e^{-\frac{(R-\overline{R})^2}{2\sigma^2}} \tag{6}$$

the PDI is equal to σ. In the cumulant method, the mean radius $\overline{R}_{cum}$ is calculated from the characteristic time τ_D in Eq. 5 using Eqs. 2 and 3. $\overline{R}_{cum}$ is therefore a harmonic average (usually called Z-average). For an extremely narrow monomodal distribution, $\overline{R}_{cum}$ is equal to the average radius from the size distribution $\overline{R}$, but with even a small polydispersity, $\overline{R}_{cum}$ is smaller than $\overline{R}$. In general, the cumulant method is considered useful only if the distribution is relatively monodisperse (i.e. PDI $\lesssim 0.5$).

When the polydispersity is larger, other types of analysis are required. The correlation function $g_1(\tau)$ is, as explained above, the sum of exponentials corresponding to the different sizes of particles present in the dispersion. The size distribution can therefore in principle be obtained by taking the Laplace transform of this correlation function. Unfortunately, and unlike the Fourier Transform, a Laplace transform is very sensitive to noise and fast and efficient algorithms do not exist. Some instruments allow using an inversion method named CONTIN. This well-documented computation routine utilizes regularized non-negative least-squares techniques combined with eigenfunction

analysis. As there is no unique answer to the inversion problem, CONTIN chooses the least detailed distribution consistent with the data. It assumes in particular that sharp peaks are improbable, so the analysis will in general broaden the distribution for extremely monodisperse particles. In addition, because of the noise problem, the quality of the correlation function data needs to be excellent in order to retrieve the actual size distribution. In this case, it has been shown that even complex multimodal distributions can be retrieved (Ostrowsky et al., 1981). Each DLS instrument uses its own improved inversion routine. It is usually recommended to measure the correlation function up to 10^4 times τ_D in order to be able to analyse the data with sophisticated routines such as CONTIN. It is -on the other hand- essential to discard the data for times much longer than τ_D if a cumulant analysis is performed.

2.3. Anisotropic particles

Light scattering instruments equipped with goniometers to vary the scattering angle are able to determine not only the mean particle size, but also the shape when the particles are large enough ($R > 10$ nm). These instruments use a combination of the gyration radius R_g, determined from the angular variation of the static scattered intensity, and of the hydrodynamic radius R_h, determined from classical DLS. R_g can be calculated plotting the static scattered intensity I as a function of q^2, $I(q) \approx 1\text{-}(q\,R_g)^2/3$ for $qR_g << 1$ and for dilute particle dispersions (Berne and Pecora, 2000).

If we take the example of rods of length L and circular section of radius r with large aspect ratio (Doi and Edwards, 1986):

$$R_g = \left(\frac{L^2}{12} + \frac{r^2}{2}\right)^{1/2} \tag{7}$$

$$R_h = \frac{L}{2\ ln\left(\frac{L}{2r}\right)} \tag{8}$$

R_g and R_h depend on L and r in different ways, hence their measurement allow the determination of both L and r.

Another method makes use only of the intensity correlation function. When particles are not spherical, their rotation also gives rise to light scattering and to a spectral broadening related to the rotational diffusion coefficient D_{rot}. The addition of a polarizer positioned between the sample and the detector enables selective collection of either the vertically polarized scattering (VV) or the horizontally depolarized scattering (VH). The corresponding field correlation functions are (Shetty et al., 2009):

$$g_{1VV}(\tau) = A\exp(-\tau/\tau_{VV}) = A\exp(-Dq^2\tau) \tag{9}$$

$$g_{1VH}(\tau) = A\exp(-\tau/\tau_{VH}) = A\exp(-(Dq^2 + 6D_{rot})\tau), \tag{10}$$

In some particular cases, two relaxations can be observed in the VV autocorrelation, and:

$$g_{1VV}(\tau) = A_1\exp(-Dq^2\tau) + A_2\exp(-(Dq^2 + 6D_{rot})\tau) \tag{11}$$

where A_1, A_2 and A are amplitudes (Glidden and Muschol, 2012) (Lee et al., 2014). Again for the example of rod-like particles (Doi and Edwards, 1986):

$$D = \frac{k_B T}{3\pi\eta L}\ln\frac{L}{2r} \tag{12}$$

$$D_{rot} = \frac{3k_B T}{\pi\eta L^3}\ln\frac{L}{4r} \tag{13}$$

Other expressions have been proposed (Brenner, 1974), but they do not differ much at large aspect ratio.

3. Results for spherical particles with small polydispersity

We will discuss examples of measurements done with polystyrene particles coated by amine groups, called afterwards PS-NH_2 particles. These particles, nominally 50 nm PS-NH_2 nanoparticles were obtained as an aqueous dispersion (Bangs Laboratories PA02 N-8626) and were used for a small Round Robin test between three different laboratories. The starting dispersion was diluted to a concentration of 1 mg/ml in MilliQ grade water and aliquots of the same dispersion were distributed to the different laboratories. For the measurement, the particle dispersions were further diluted in pure water by a factor ten in each laboratory to reach a final concentration of 100 μg/ml. The sample preparation and the measurement were performed following a standard operating procedure (SOP) established within the EU funded Research Infrastructure QualityNano (Langevin et al., 2018).

The measurements have been done using four different DLS instruments that were randomly selected to have different instrumental set-ups as examples in our study. As the goal was not to compare different vendors, but to highlight potential issues and provide suggestions applicable to any DLS instrument, the results are given using instrument numbers 1–4 (without specifying the origin of the instruments). The scattering angle in instruments 1–3 is fixed to 173°; the light sources are either LEDS or lasers with λ ~650 nm and avalanche photodiode detectors are used. Instrument 4 is equipped with a goniometer and experiments were performed at various angles θ = 40, 60, 90 and 120°. This setup works with a He-Ne laser (λ = 632.8 nm). The temperature was set at 25 °C.

The measured sizes and PDIs are reported in Table 1. The numbers are averages of experiments made three times, each with three different samples. The error bars for the cumulant analysis correspond to the standard deviation over these nine measurements.

The experiments done with instruments 1, 2 and 4 are fully consistent (diameter 58 nm, PDI < 10%). A simple exponential fit of the correlation function was performed with instrument 4, as it is known that PDI values < 10% can hardly be measured using DLS. Furthermore, experiments at several scattering angles were performed and the average taken. As explained earlier, this procedure leads to more reliable results, since the angular dependence can be used to verify that the particles undergo a diffusion process. As a result, the standard deviation is larger than with instruments 1 and 2, because it accounts for the repeatability of measurements while the scattering angle is varied.

DLS instruments allow in general not only an analysis by the cumulant method, but also by inversion methods such as CONTIN. When using the inversion methods, the results are different, the diameter and the PDIs are systematically larger (see Table 1). Possible reasons for this difference were discussed in §2 (noise level, intrinsic software artifacts).

The diameters and PDIs obtained with instrument 3 are compatible, although slightly larger. The cumulant analysis leads to a mean diameter of 66 nm and a significantly larger PDI: 0.23. The PDI significantly varies from one measurement to another, from 0.07 to 0.50. This is accompanied by a large variation of the average diameter, between 61 and 76 nm. Fig. 1 shows the size distributions obtained with the inversion method, where the spread in diameters is still larger (66

Table 1
Measured sizes and polydispersities of the PS-NH2 nanoparticles from the different instruments obtained using different analysis procedures.

Laboratory	Diameter, nm (cumulants)	PDI (cumulants)	Diameter, nm (inversion method)	PDI (inversion method)
Instrument 1	58.0 ± 0.2	0.06 ± 0.01	61.2 ± 0.3	0.28 ± 0.10
Instrument 2	59.6 ± 0.4	0.06 ± 0.01	64.3 ± 0.5	0.28 ± 0.15
Instrument 3	66 ± 6	0.23 ± 0.15	95 ± 26	0.76 ± 0.50
Instrument 4	58 ± 2	< 0.1		

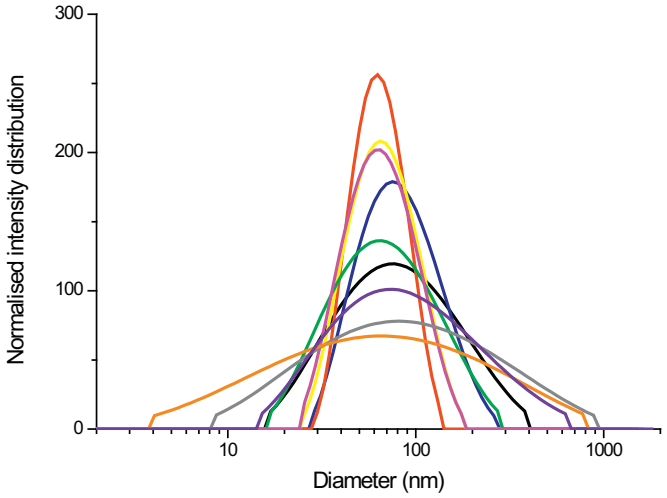

Fig. 1. Diameter distributions (intensity averaged) of PS-NH_2 particles obtained by instrument 3 (the nine curves corresponds to the nine experiments, see text). The distributions plotted are obtained from a CONTIN analysis.

to 144 nm).

In order to find the possible origin of these discrepancies, we have looked in more detail at the correlation function $g_2(\tau)$ obtained with the instrument 3. We selected one of the 9 experiments for which the cumulant analysis led to a diameter of 61.2 nm and a PDI of 0.123. The correlation function $g_2(\tau)$ was measured for τ between 0 and 1 s, although the main decrease occurs during the first millisecond. It is therefore possible that the noise introduced by non-significant data at large t produces artifacts in the fitting procedure. We have therefore kept only the data between 1 and 400 μs (Fig. 2). Above 400 μs, $g_2(\tau)$ is equal to 1 within $< 10^{-2}$ and some values of g_2–1 are negative; in this case, ln (g_2–1) is not defined and no fit can be performed. The instrument's software suppresses data points, but one has to specify a minimum value for g_2, usually set at 1.003. Note that in our fits, we have cut all the points above $\tau = 400$ μs, and g_2 was always larger than 1. In the data used by the instrument, g_2 values of 1.003 are found already for times as short as 3800 μs.

Two fits were performed for ln [$g_2(\tau)$-1], a linear fit and a polynomial (cumulant) fit using Eqs. 1 and 5. They are shown in Fig. 2. It is observed that the linear fit and the polynomial fit are indistinguishable from one another. This is more evident in the inset, restricted to short times, 1–30 μs. It is also noticed that the noise in the data prevents a safe determination of the PDI. In the case discussed, the PDI obtained from the cumulant fit is 0.025, much lower than the value given by the instrument with the same cumulant analysis. The correlation time from this fit leads to a diameter of 60 ± 1.3 nm, somewhat smaller than the value given by the instrument, but consistent with those obtained with the other instruments (Table 1). Note that the error bar obtained for the fit of data from instrument 4 corresponds to the scatter of correlation function data points, and that this error is not provided by the other instruments. The errors quoted in Table 1 correspond to the variations from one experiment to another, the actual error being probably somewhat larger. The mean diameter found with our analysis is smaller than the diameter indicated by the instrument, because of the different ways in which data points are removed. When $g_2 < 1.0003$, the instrument replaces the actual value of g_2 by 1.0003, introducing therefore many large values of g_2; this artificially increases the correlation time and, as a consequence, the particle diameter.

This discussion demonstrates that a poor signal to noise ratio

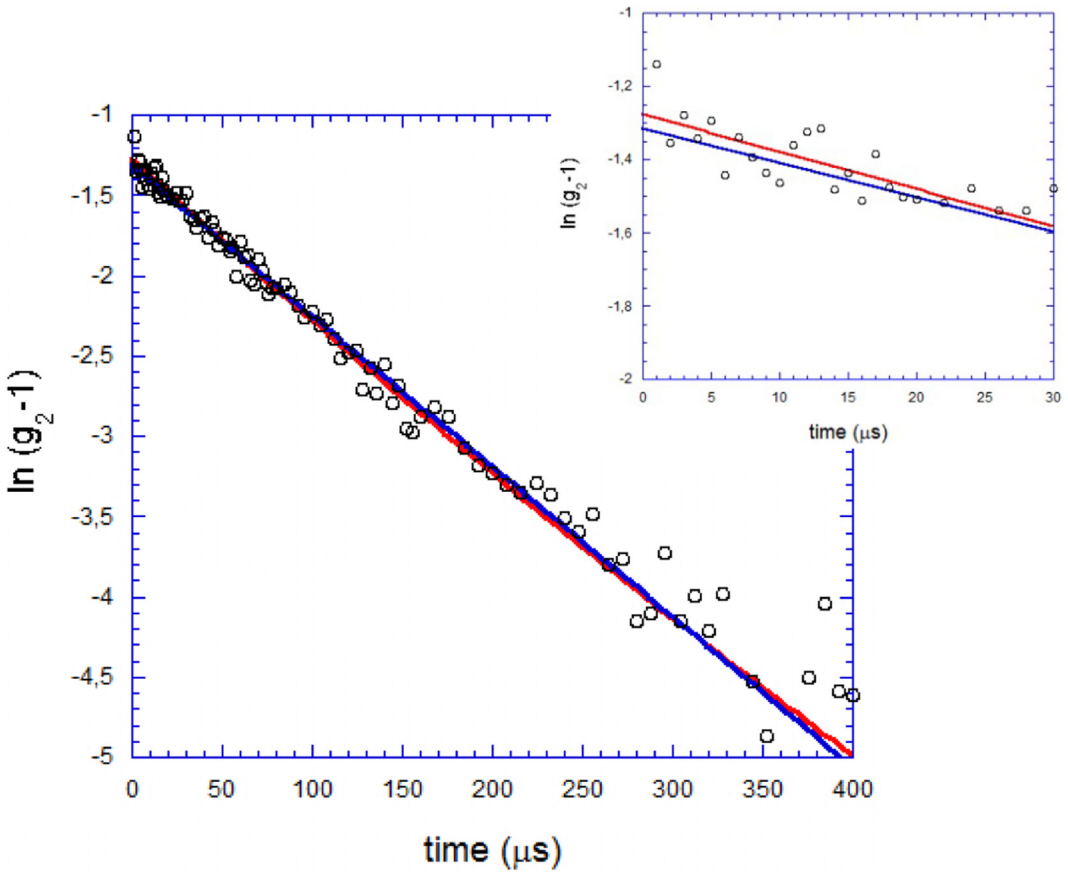

Fig. 2. Correlation function measured for lag times τ of up to 400 μs. The fits are shown by blue, for the linear, and red for the cumulant. Inset: Correlation functions at shorter times, up to 30 μs.

introduces important uncertainties in the determination of the correlation time distribution. It confirms that the cumulant method cannot be safely used without cutting data at times much longer than τ_D. The noise introduces errors in the size distribution and as a consequence, errors in the measured sizes. The problem arises with all instruments when the samples are diluted too much.

As shown above, the results from cumulant analysis depend on the selected range of delay times and the number of data points. Whenever possible, it is preferable to use the modified version of the standard cumulant analysis proposed by Frisken (Frisken, 2001). This modified version is less sensitive to noise in the baseline and results in more robust fitting in general.

DLS instruments may also provide the size distribution by number and by intensity when an inversion analysis is performed. As we have mentioned earlier, these distributions should be handled with caution as the size averages and the polydispersity increase when the noise level increases. For instance, with the rather monodisperse PS-NH2 particles studied, the intensity averaged diameter is 64 nm, while the number average is only 44 nm. This allows comparing the size with measurements from electron microscopy images. As the intensity is proportional to the square of the particle volume, intensity averages are shifted to large diameter values with respect to number averages.

4. Results for very polydisperse particles

The intensity of the light scattered by particles increases as the sixth power of their diameter. Therefore, the signal is in general dominated by the largest particles. When the dispersions contain both large and small particles, the small ones are difficult to detect.

An example is given in Fig. 3 with titanium oxide nanoparticles dispersed in a phosphate buffer. The TiO_2 nanoparticles used were purchased from Evonik (AEROXIDE® TiO_2 P25). The diameter of these particles is 21 nm. They were first dispersed by sonication in ultrapure water, at 21 °C. The final solutions, at concentrations between 0.6 and 13 mg/ml were prepared in saline phosphate buffered (PBS 10×, Gibco #7011-036). The ionic strength of the buffer is large (around 0.1 M), which leads to partial agglomeration of the particles. Regardless their concentration, large agglomerates were detected. A number distribution, averaged over 9 measurements is shown in Fig. 3.

The instrument indicated that the results do not meet quality criteria: the polydispersity is too high for distribution analysis and even for cumulant analysis. Interestingly, experiments were performed on the same samples using a different method, differential centrifugal sedimentation (DCS) (Lozano et al., 2012; Mejia et al., 2013) and the distribution obtained was centered on the nominal size of 21 nm. DCS is a technique based on the use of centrifugal force on a spinning disk to fractionate samples by size and density, performing the measurements with a laser source almost at the end of the disk. For a sample with multiple populations of the same material (hence the same density), the sample will be fractionated by populations, ensuring the hydrodynamic measurement of each population individually. This result confirms that the original small particles are still present and that the amount of aggregates is much less than suggested by Fig. 3, even when calculated number distributions are plotted.

This example illustrates the limitations of standard DLS, clearly not appropriate to characterize partially agglomerated particles. Electron microscopy, particle tracking analysis and tunable resistive pulse sensors are other methods that, as DCS, are less sensitive to polydispersity (Anderson et al., 2013). Thus for partially agglomerated particles or polydisperse samples, DLS should be used in combination with one of these methods in order to assess the validity of the measurements. Note that this example was selected to illustrate potential problems. In cell culture media, agglomeration of nanoparticles can be detectable but less pronounced, in which cases particle size determination is possible (Langevin et al., 2018).

5. Results for non-spherical particles

Light scattering instruments equipped with goniometers in order to vary the scattering angle are able to determine not only the mean particle size, but also the shape when the particles are large enough ($R > 10$ nm) and not too polydisperse. These instruments use a combination of the gyration radius R_g and of the hydrodynamic radius R_h as discussed in Section 2.

Another method makes use only of the intensity correlation function, but for polarized and depolarized scattering. The method allows the determination of both rotational, D_{rot}, and translational, D, diffusion coefficients. Measurements at several angles are usually necessary to separate the translational (q dependent) and rotational (q independent) contributions (see Eqs. 9). Experiments have been performed with nanotube dispersions by Shetty et al. who used a commercial instrument equipped with a goniometer and added a polarizer (Shetty et al., 2009).

We show below an example of this method. We measured the polarized (VV) and depolarized (VH) dynamic light scattering using a light scattering setup equipped with a goniometer, on which two Glan-Taylor polarizing prisms (CVI Melles Griot, France) were mounted. The

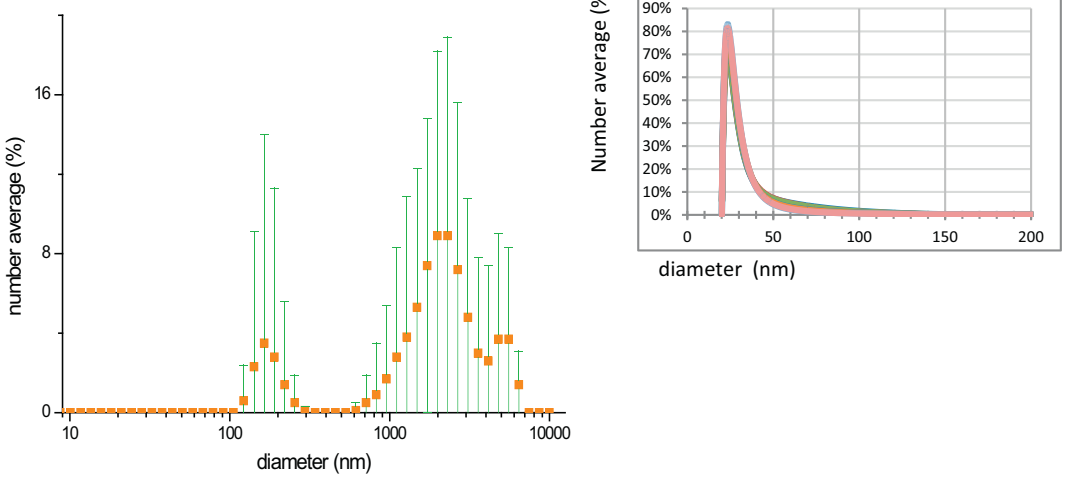

Fig. 3. Number distribution of TiO_2 particles dispersed in a phosphate buffer as deduced from CONTIN analysis of DLS data. Inset: distribution obtained with the DCS technique with the same samples.

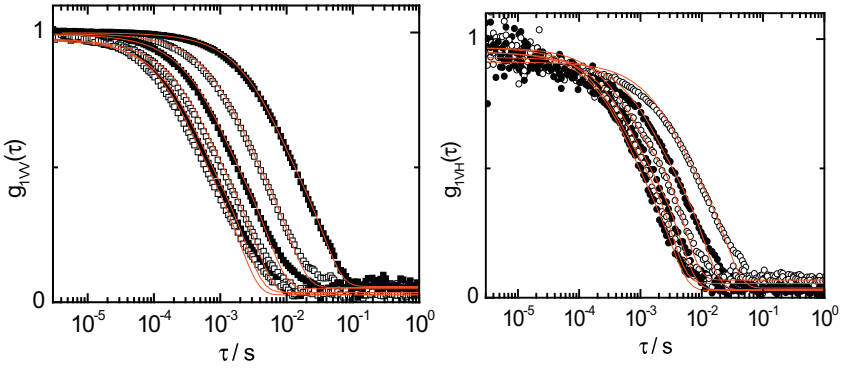

Fig. 4. Correlation functions g_{1VV} and g_{1VH} at scattering angles θ = 30, 50, 70, 90, 110, 130°.

nanotubes used were functionalized by the method of (Shetty et al., 2009) in order to disperse them in water. The polarized and depolarized electric field correlation functions $g_{1VV}(q,t)$ and $g_{1VH}(q,t)$ are shown in Fig. 4. We fitted these autocorrelation functions with an exponential decay and a first order cumulant term (Eq. 5).

The characteristic relaxation times τ_{VV} and τ_{VH} are such that: $1/\tau_{VV} = D\,q^2$ and $1/\tau_{VH} = D\,q^2 + 6D_{rot}$ (see Eqs. 9 and 10). The slope of $1/\tau_{VV}$ versus q^2 leads to $D = 1.88\ 10^{-12}$ m^2/s, fixing D and extrapolating $1/\tau_{VH}$ to $q^2 = 0$ leads to $6D_{rot} = 63.0\ s^{-1}$ (see Fig. 5).

D and D_{rot} permit to calculate the length L and the radius r of the nanotube following Eqs. 12 and 13. One finds: $r = 1.8 \pm 1$ nm and $L \sim 1.3$ µm. The PDI is large, around 0.6, likely because of the polydispersity in length of the nanotubes. AFM or SEM images of similar nanotubes gave L values between 500 and 1500 nm (Knyazev et al., 2011), in good agreement with the value measured here. The determination of r is the less precise, because it appears in a logarithm in Eqs. 12 and 13. The mean r value is slightly larger than that measured with AFM: $r = 1 \pm 0.2$ nm (Campidelli et al., 2008), but the agreement is reasonable in view of the error bars.

Usually, measurements at a number of scattering angles are necessary to separate the contributions of translation (q dependent) and rotation (q independent). Gold nanorods were also studied with a depolarized DLS instrument (Glidden and Muschol, 2012). Interestingly, the authors made a comparison with an instrument without polarizers that essentially collects VV data. They used CONTIN distributions which were bimodal, and identified the two peaks with the relaxations predicted by Eq. 11. The results were consistent with those obtained by the first instrument. This good agreement of course relies on the monodispersity of the rods, as we have seen that cumulant and CONTIN analysis do not give exactly the same results, even for rather monodisperse and spherical particles (differences of order 5%, see Table 1). Similar experiments were performed with non-spherical gold-platinum Janus nanoparticles (Lee et al., 2014). Note that for these strongly asymmetric particles mistakes in the analysis could be made if the two relaxations are interpreted as a distribution of two size populations.

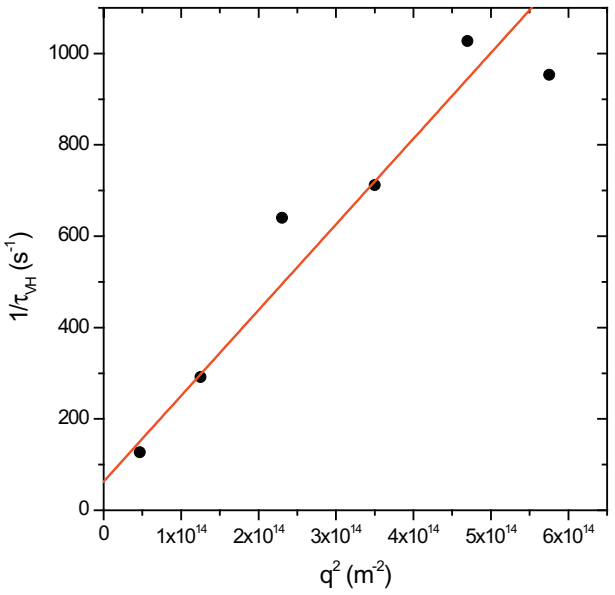

Fig. 5. Variation of $1/\tau_{VH}$ with q^2. The line is the fit with $1/\tau_{VH} = D\,q^2 + 6D_{rot}$ using the diffusion coefficient D determined from τ_{VV}.

These methods can of course be applied to other types of anisotropic particles. Relations between R_g and R_h or R_h and D_{rot} have been established for other types of particles. In the case of specific shapes, they can also be computed (Garcia de la Torre et al., 1994).

6. Recommendations to minimize errors

Here we would like to summarize the most important take home messages and recommendations for reliable size measurements using DLS, applicable to any DLS instrument. Even when measuring rather monodisperse spherical particles care has to be taken to obtain correct results.

- Most instruments propose different methods of analysis (cumulant, CONTIN). One could first check if results obtained with the different methods are in agreement with each other. We have seen that in the example chosen, different methods of analysis gave different results. When this occurs it is preferable to use the values given by the cumulant method which are less sensitive to noise.
- In the case of a cumulant analysis, and in order to limit the possible influence of the noise in the data treatment, the range of correlation times investigated should be limited, typically to times above which the correlation function has decreased by a factor of 100. Setting a lower limit for g_2 and using a larger range of correlation times introduces errors.
- An important parameter is the minimum detected intensity below which the measurements are not reliable. DLS instruments frequently indicate when the intensity is too low, and the difficulty can sometimes be overcome by removing attenuators. When this is not possible, one can in principle increase the time of acquisition, so simply measure for a longer time. It is our experience, however, that in this case in general the signal often does not significantly improve even after long averaging. The best solution in general is to increase the particle concentration.
- Some instruments are not very strict with the corresponding noise level. In case of doubt, the intensity can be varied by changing the optical filters or the size of the detection pinhole. If the intensity range is appropriate, the sizes measured should not change.

Sonication is a usual step in the preparation of the dispersions and

helps to break the agglomerates eventually formed. In order to ensure repeatability of the measurements, it is useful to calibrate the sonication energy (DeLoid et al., 2017). Other sources of error could be:

- Some instruments automatically adapt the position of the cell. It is important to verify that the light beam does not travel across the meniscus if the liquid volume in the cell is too small
- In general, glass cells or plastic cells are used for DLS measurements. If the particles adsorb onto glass or plastic, the results will not be reliable.

In the general case, and even for spherical particles, it is quite useful to perform measurements at different scattering angles (when the instrument allows it) and different concentrations; extrapolations to zero allow measuring more accurately the diffusion coefficients and they can also provide additional information, such as interparticle interactions (using Eq. 4). In the case of anisotropic particles, we have shown that also fixed angle instruments provide reliable results for monodisperse rods. For all cases and regardless the shape of the particles, when the polydispersity becomes high, relying on DLS alone becomes difficult and combination with additional technique(s) becomes necessary.

7. Conclusion

Dynamic light scattering is a very versatile technique for analyzing the particle size based on the study of Brownian motion of nanoparticles in a liquid medium. Although its main application is for particle sizing, it is important to remember that DLS is not accurate for polydisperse samples: particles of larger sizes scatter light more efficiently, hence the scattering is dominated by the fraction of particles of larger size. The average size is therefore shifted with respect to the size measured for instance by electron microscopy. DLS results from polydisperse samples should be considered as indicative, especially those obtained with inversion methods.

Other significant errors could be made when working with dilute dispersions or very small particles that scatter little light. When the instruments allow retrieving the correlation function data, the results can be analyzed in more detail, taking into account the actual noise of the correlation functions, and in this way better estimations of the sizes can be made.

Finally, one of the great advantages of the DLS technique is the possibility to obtain additional information, for instance on hydrodynamic interactions between particles when their concentration is sufficient (volume fractions above a few percent). Anisotropic particles cause depolarization of the scattered light and when using polarizers, also information about shape can be obtained.

In the case of particles of arbitrary shapes, it is difficult to assess their precise shape using light scattering only. As when the polydispersity is very high, combinations with other techniques is recommended.

Acknowledgements

The work presented here has been supported by the EU FP7 Capacities project QualityNano (grant no. INFRA-2010-262163) and the FP7 project FutureNanoNeeds (grant no. 604602).

References

Anderson, W., et al., 2013. A comparative study of submicron particle sizing platforms: accuracy, precision and resolution analysis of polydisperse particle size distributions. J. Colloid Interface Sci. 405, 322–330.
Anguissola, S., et al., 2014. High content analysis provides mechanistic insights on the pathways of toxicity induced by amine-modified polystyrene nanoparticles. PLoS One 9 (9), e108025.
Beltran-Huarac, J., et al., 2018. Development of reference metal and metal oxide engineered nanomaterials for nanotoxicology research using high throughput and precision flame spray synthesis approaches. NanoImpact 10, 26–37.
Berne, B.J., Pecora, R., 2000. Dynamic Light Scattering: With Applications to Chemistry, Biology, and Physics. Dover Publications.
Brenner, H., 1974. Rheology of a dilute suspension of axisymmetric Brownian particles. Int. J. Multiphase Flow 1 (2), 195–341.
Campidelli, S., et al., 2008. Facile decoration of functionalized single-wall carbon nanotubes with phthalocyanines via “Click Chemistry”. J. Am. Chem. Soc. 130 (34), 11503–11509.
De Matteis, V., et al., 2015. Negligible particle-specific toxicity mechanism of silver nanoparticles: the role of Ag+ ion release in the cytosol. Nanomedicine 11 (3), 731–739.
DeLoid, G.M., et al., 2017. Preparation, characterization, and in vitro dosimetry of dispersed, engineered nanomaterials. Nat. Protoc. 12, 355.
Doi, M., Edwards, S.F., 1986. The Theory of Polymer Dynamics. Oxford University Press, New York.
Frisken, B.J., 2001. Revisiting the method of cumulants for the analysis of dynamic light-scattering data. Appl. Opt. 40 (24), 4087–4091.
Garcia de la Torre, J., et al., 1994. HYDRO: a computer program for the prediction of hydrodynamic properties of macromolecules. Biophys. J. 67 (2), 530–531.
Glidden, M., Muschol, M., 2012. Characterizing gold nanorods in solution using depolarized dynamic light scattering. J. Phys. Chem. C 116 (14), 8128–8137.
Guarnieri, D., et al., 2014. Transport across the cell-membrane dictates nanoparticle fate and toxicity: a new paradigm in nanotoxicology. Nano 6 (17), 10264–10273.
Kerker, M., 1969. The Scattering of Light and Other Electromagnetic Radiation. Academic Press.
Knyazev, A., et al., 2011. Selective adsorption of proteins on single-wall carbon nanotubes by using a protective surfactant. Chem Eur J 17 (51), 14663–14671.
Langevin, D., et al., 2018. Inter-laboratory comparison of nanoparticle size measurements using dynamic light scattering and differential centrifugal sedimentation. NanoImpact 10, 97–107.
Lee, T.C., et al., 2014. Self-propelling nanomotors in the presence of strong Brownian forces. Nano Lett. 14 (5), 2407–2412.
Lozano, O., et al., 2012. Effects of SiC nanoparticles orally administered in a rat model: biodistribution, toxicity and elemental composition changes in feces and organs. Toxicol. Appl. Pharmacol. 264 (2), 232–245.
Mejia, J., et al., 2013. Dose assessment of SiC nanoparticle dispersions during in vitro assays. J. Nanopart. Res. 15 (8).
Nel, A.E., et al., 2009. Understanding biophysicochemical interactions at the nano-bio interface. Nat. Mater. 8 (7), 543–557.
Ostrowsky, N., et al., 1981. Exponential sampling method for light-scattering polydispersity analysis. Opt. Acta 28 (8), 1059–1070.
Russel, W.B., 1981. Brownian-motion of small particles suspended in liquids. Annu. Rev. Fluid Mech. 13, 425–455.
Russo, P., 2012. http://macro.lsu.edu/howto/DLS_Minicourse/DLS_Minicourse.pdf.
Sabella, S., et al., 2014. A general mechanism for intracellular toxicity of metal-containing nanoparticles. Nano 6 (12), 7052–7061.
Shetty, A.M., et al., 2009. Multiangle depolarized dynamic light scattering of short functionalized single-walled carbon nanotubes. J. Phys. Chem. C 113 (17), 7129–7133.
Wang, F., et al., 2013. Time resolved study of cell death mechanisms induced by amine-modified polystyrene nanoparticles. Nano 5 (22), 10868–10876.
Zhang, H., et al., 2012. Processing pathway dependence of amorphous silica nanoparticle toxicity: colloidal vs pyrolytic. J. Am. Chem. Soc. 134 (38), 15790–15804.

Update

NanoImpact

Volume 21, Issue , January 2021, Page

DOI: https://doi.org/10.1016/j.impact.2020.100286

NanoImpact 21 (2021) 100286

Contents lists available at ScienceDirect

NanoImpact

journal homepage: www.elsevier.com/locate/nanoimpact

Erratum regarding missing Declaration of Competing Interest statements in previously published articles

The Declaration of Competing Interest statements were not included in the published version of the following articles that appeared in previous issues of NanoImpact. The appropriate Declaration\Competing Interest statements, provided by authors, are included below.

1. "New tools in risk assessment of nanomaterials" (NanoImpact, 2019; 16C: 100189) doi:https://doi.org/10.1016/j.impact.2019.100189 (web archive link,) Declaration of competing interest: The authors declare that they have no known competing financial interests or personal relationships that could have appeared to influence the work reported in this paper.
2. "Reliability of methods and data for regulatory assessment of nanomaterial risks" (NanoImpact, 2018; 10C: 68–69) doi:https://doi.org/10.1016/j.impact.2017.11.005 (web archive link,) Declaration of competing interest: The authors declare that they have no known competing financial interests or personal relationships that could have appeared to influence the work reported in this paper.
3. "Depletion of double-layer coated nano-TiO2 and generation of reactive oxygen species in the presence of ethanol under simulated solar irradiation" (NanoImpact, 2018; 11C: 164–169) doi:https://doi.org/10.1016/j.impact.2018.08.004 (web archive link,) Declaration of competing interest: The authors were contacted after publication to request a Declaration of Interest statement.
4. "Ecotoxicity screening of seven different types of commercial silica nanoparticles using cellular and organismic assays: Importance of surface and size" (NanoImpact, 2019; 13C: 100–111) doi:https://doi.org/10.1016/j.impact.2019.01.001 (web archive link,) Declaration of competing interest: The authors were contacted after publication to request a Declaration of Interest statement.
5. "Towards reproducible measurement of nanoparticle size using dynamic light scattering: Important controls and considerations" (NanoImpact, 2018; 10C: 161–167) doi:https://doi.org/10.1016/j.impact.2018.04.002 (web archive link,) Declaration of competing interest: The authors declare that they have no known competing financial interests or personal relationships that could have appeared to influence the work reported in this paper.
6. "Abiotic dissolution rates of 24 (nano)forms of 6 substances compared to macrophage-assisted dissolution and in vivo pulmonary clearance: Grouping by biodissolution and transformation" (NanoImpact, 2018; 12C: 29–41) doi:https://doi.org/10.1016/j.impact.2018.08.005 (web archive link,) Declaration of competing interest: The authors declare the following financial interests/personal relationships which may be considered as potential competing interests: JKJ, JGK, KW, PM, LMH, RL, WW are employees of BASF SE, a company producing and marketing nanomaterials. AV and MW declare no competing interests.
7. "Thermal decomposition/incineration of nano-enabled coatings and effects of nanofiller/matrix properties and operational conditions on byproduct release dynamics: Potential environmental health implications" (NanoImpact, 2018; 13C: 44–55) doi:https://doi.org/10.1016/j.impact.2018.12.003 (web archive link,) Declaration of competing interest: The authors were contacted after publication to request a Declaration of Interest statement.
8. "Single platform spin-spin nuclear relaxation time (1H NMR) based technique for assessing dissolution and agglomeration of CuO nanoparticles" (NanoImpact, 2019; 14C: 100148) doi:https://doi.org/10.1016/j.impact.2019.100148 (web archive link,) Declaration of competing interest: The authors declare that they have no known competing financial interests or personal relationships that could have appeared to influence the work reported in this paper.
9. "A systematic process for identifying key events for advancing the development of nanomaterial relevant adverse outcome pathways" (NanoImpact, 2019; 15C: 100178) doi:https://doi.org/10.1016/j.impact.2019.100178 (web archive link,) Declaration of competing interest: The authors declare that they have no known competing financial interests or personal relationships that could have appeared to influence the work reported in this paper.
10. "Release of radiolabeled multi-walled carbon nanotubes (14C-MWCNT) from epoxy nanocomposites into quartz sand-water

DOIs of original article: https://doi.org/10.1016/j.impact.2019.100148, https://doi.org/10.1016/j.impact.2019.100176, https://doi.org/10.1016/j.impact.2018.08.005, https://doi.org/10.1016/j.impact.2019.100189, https://doi.org/10.1016/j.impact.2018.12.003, https://doi.org/10.1016/j.impact.2019.100178, https://doi.org/10.1016/j.impact.2019.100159, https://doi.org/10.1016/j.impact.2017.11.005, https://doi.org/10.1016/j.impact.2019.01.001, https://doi.org/10.1016/j.impact.2018.04.002, https://doi.org/10.1016/j.impact.2018.12.001, https://doi.org/10.1016/j.impact.2018.06.003, https://doi.org/10.1016/j.impact.2018.08.004, https://doi.org/10.1016/j.impact.2019.100161, https://doi.org/10.1016/j.impact.2018.06.002.

https://doi.org/10.1016/j.impact.2020.100286

Available online 15 December 2020

systems and their uptake by Lumbriculus variegatus" (NanoImpact, 2019; 14C: 100159) doi:https://doi.org/10.1016/j.impact.2019.100159 (web archive link,) Declaration of competing interest: The authors were contacted after publication to request a Declaration of Interest statement.

11. "Differential physiological and biochemical impacts of nano vs micron Cu at two phenological growth stages in bell pepper (Capsicum annuum) plant" (NanoImpact, 2019; 14C: 100161) doi:https://doi.org/10.1016/j.impact.2019.100161 (web archive link,) Declaration of competing interest: The authors were contacted after publication to request a Declaration of Interest statement.
12. "Nanosilver: An innovative paradigm to promote its safe and active use" (NanoImpact, 2018; 11C: 128–135) doi:https://doi.org/10.1016/j.impact.2018.06.003 (web archive link,) Declaration of competing interest: The authors were contacted after publication to request a Declaration of Interest statement.
13. "Toward a better extraction of titanium dioxide engineered nanomaterials from complex environmental matrices" (NanoImpact, 2018; 11C: 119–127) doi:https://doi.org/10.1016/j.impact.2018.06.002 (web archive link,) Declaration of competing interest: The authors declare that they have no known competing financial interests or personal relationships that could have appeared to influence the work reported in this paper.
14. "SUNDS probabilistic human health risk assessment methodology and its application to organic pigment used in the automotive industry" (NanoImpact, 2018; 13C: 26–36) doi: https://doi.org/10.1016/j.impact.2018.12.001 (web archive link,) Declaration of competing interest: The authors were contacted after publication to request a Declaration of Interest statement.
15. "A 21-day sub-acute, whole-body inhalation exposure to printer-emitted engineered nanoparticles in rats: Exploring pulmonary and systemic effects" (NanoImpact, 2019; 15C: 100176) doi:https://doi.org/10.1016/j.impact.2019.100176 (web archive link,) Declaration of competing interest: The authors were contacted after publication to request a Declaration of Interest statement.